Probing the Structure of the Cytoplasmic Domain of the Aspartate Receptor by Targeted Disulfide Cross-Linking[†]

Xiaomin Chen[‡] and Daniel E. Koshland, Jr.*

Department of Molecular and Cell Biology, University of California, Berkeley, California 94720

Received April 21, 1997; Revised Manuscript Received June 25, 1997[⊗]

ABSTRACT: Applying the technique of targeted disulfide cross-linking to the cytoplasmic domain of the aspartate receptor of *Salmonella typhimurium* indicates a generally α-helical conformation of the linker region, and a close juxtaposition and a parallel alignment at the interface between the two subunits in the linker region. This conclusion is supported by the results from the Fourier transform of the hydrophobicity values of the amino acid sequences. Aspartate binding in the periplasmic domain causes a closer juxtaposition of the two subunits in the cytoplasmic domain, as indicated by the more rapid disulfide cross-linking on addition of aspartate.

The aspartate receptor mediates bacterial chemotaxis to aspartate and some repellents in *Escherichia coli* and *Salmonella typhimurium*. It is a dimeric inner membrane protein with two identical subunits (Milligan & Koshland, 1988). The molecule has two periplasmic recognition domains and two cytoplasmic signaling domains, connected by four transmembrane segments called TM 1 and TM 2 in one subunit and TM 1′ and TM 2′ in the other. The aspartate receptor belongs to a family of receptors, including insulin receptor, EGF receptor, LDL receptor, cytokine receptors, and the chemotactic receptors, which all have one or two transmembrane segments per subunit in a functional dimer (Lee & Pilch, 1994). They often have similar mechanisms of transmembrane signaling because a hybrid insulin-aspartate receptor has been shown to be functional (Moe et al., 1989; Biemann et al., 1996).

Among the biophysical and biochemical approaches to study membrane proteins, targeted disulfide cross-linking has been extremely valuable to delineate their structure−function relationships. It was first applied to this receptor to define its domain structure, surface accessibility and spatial proximity of some residues (Falke & Koshland, 1987). It was also found that the receptor that was cross-linked at 36−36′ was functional in transmembrane signaling (Milligan & Koshland, 1988). The 36−36′ disulfide bond made it possible to crystallize the periplasmic domain (Jancarik et al., 1991), and the results helped discover conditions for the crystallization of the non-cross-linked wild type (Yeh et al., 1993). The structure of the cross-linked periplasmic domain was determined to high resolution (Milburn et al., 1991; Yeh et al., 1993). Transmembrane segments have been delineated by similar cross-linking experiments (Lynch & Koshland, 1991; Stoddard et al., 1992). Similar studies have been done on the transmembrane regions of other proteins, such as the *E. coli* ribose/galactose receptor Trg (Lee et al., 1994, 1995a,b), lactose permease (Sahin-Toth & Kaback, 1993; Weitzman & Kaback, 1995), and the aspartate receptor (Pakula & Simon, 1992).

Targeted disulfide cross-linking has also helped us in understanding the signaling mechanism of the aspartate receptor. The cross-linking studies between TM1 and TM1′ indicates that these helices did not move relative to each other when aspartate binds (Lynch & Koshland, 1992; Stoddard et al., 1992). This agrees with a model of helices 4 and 4′ moving in a piston motion (Mowbray & Koshland, 1987; Lynch & Koshland, 1992) when aspartate is added. Cross-linked dimers have been constructed containing a mixture of truncated and full-length subunits that indicated that signaling occurs via conformational changes in which the message to the cytoplasm was transduced through a single subunit (Milligan & Koshland, 1991). The results have been confirmed by genetic studies (Gardina & Manson, 1996; Tatsuno et al., 1996).

In the studies described here, we have applied this targeted cross-linking technique to the cytoplasmic domain of the receptor. Circular dichroism (Foster et al., 1985; Wu et al., 1996) and secondary structure predictions (Le Moual & Koshland, 1996) suggested that the cytoplasmic domain had a high content of α-helical structure. Functionally, the cytoplasmic domain of the receptor can be divided into four functional regions: a methylation region including four specific glutamate residues (295, 302, 309, and 491) that are the substrates for the methyltransferase (CheR) and methylesterase (CheB), a signaling (CheW-CheA interacting) region between methylation sites 3 and 4, a "linker region" between the membrane and the first methylation site, and a methyl transferase activation region (Wu et al., 1996). The linker region of the cytoplasmic domain was chosen as the first target in this study since it connects two important functional domains: the periplasmic domain and the signaling domain (methylation region and CheW/CheA binding region), and it contains the A19K pseudorevertant region (Oosawa & Simon, 1986). This region is highly conserved, i.e., the overall sequence homology being over 70% among six different chemoreceptors [Figure 1 and Le Moual and Koshland (1996)].

[†] This work was supported by National Institutes of Health Grant DK09765 and by the W. M. Keck Foundation.

* To whom correspondence should be addressed.

[‡] Present address: Laboratories of Molecular Biophysics, The Rockefeller University, New York, NY 10021.

[⊗] Abstract published in *Advance ACS Abstracts,* September 1, 1997.

S0006-2960(97)00911-2 CCC: $14.00

	260 270 280 289
Tar_s	SLIDTVTQVREGSDAIYSGTSEIAAGNTDL
Tar_e	SLTDTVTHVREGSDAIYAGTREIAAGNTDL
Tsr_e	ELMRTVGDVRNGANAIYSGASEIATGNNDL
Trg_e	SLGMTVGTVRQGAEEIYRGTSEISAGNADL
Tap_e	ALRGTVSDVRKGSQEMHIGIAEIVAGNNDL
Tcp_s	SLIRTVSAVRDNADSIYTGAGEISAGSSDL
Identities	L TV VR G EI G DL

FIGURE 1: Amino acid sequence comparison of chemoreceptors in the linker region of *E. coli* and *S. typhimurium*. Tar_s, *S. typhimurium* aspartate receptor (Russo & Koshland, 1983); Tar_e, *E. coli* aspartate receptor (Krikos et al., 1983); Tsr_e, *E. coli* serine receptor (Boyd et al., 1983); Trg_e; *E. coli* ribose/galactose receptor (Bollinger et al., 1984); Tap_e; *E. coli* dipeptide receptor (Krikos et al., 1983); and Tcp_s, *S. typhimurium* citrate receptor (Yamamota & Imae, 1993). Identities: residues identical in all six receptors.

sequence	QRSLIDTVTQVREGSDAIYSGTSEIAAGNTDL
C	Q258C
C	R259C
C	S260C
C	L261C
C	I262C
C	D263C
C	T264C
C	V265C
C	T266C
C	Q267C
C	V268C
C	R269C
C	E270C
C	G271C
C	S272C
C	D273C
C	A274C
C	I275C
C	Y276C
C	S277C
C	G278C
C	T279C
C	S280C
C	E281C
C	I282C
C	A283C
C	A284C
C	G285C
C	N286C
C	T287C
C	D288C
C	L289C

FIGURE 2: Cysteine mutants made in this study. C is shown at position at which C was substituted for wild type amino acid.

MATERIALS AND METHODS

Materials. *E. coli* strain HCB721 (Wolfe et al., 1988) was obtained from Dr. Howard C. Berg at Harvard University. RP8611 was obtained from Dr. J. Sandy Parkinson at University of Utah. Mutagenic oligonucleotides were either from Operon or from the DNA Synthesis Facility, University of California, Berkeley. T4 Mutagene kit was from BioRAD. Cycle sequencing kit was from Gibco BRL. *S*-Adenosyl-L-[^{3}H]methionine (AdoMet) was purchased from Amersham. The methyltransferase CheR was prepared as described in Shapiro and Koshland (1994). *N*-ethylmaleimide (NEM) and other chemicals were from Sigma.

Mutant Construction. Plasmid pXCK09 (constructed by Dr. Joseph J. Falke), which has the tar_s gene (encoding the *S. typhimurium* aspartate receptor) inserted into pEMBL18, was used to prepare the ssDNA template. Cysteine mutants were made by site-directed mutagenesis according to Kunkel (1985), using a Mutagene kit. Mutations were confirmed by dsDNA PCR sequencing.

Membrane Preparation. Membrane samples were prepared from HCB721 cells, according to Chen and Koshland (1995), except that in all buffers used, DTT was added to 10 mM.

Methylation Labeling of the Aspartate Receptor. The membranes from −80 °C were thawed on ice. Then they were mixed with equal volume of methylation cocktail [1/10 volume of *S*-adenosyl-L-[^{3}H]methionine, 150 mM NaP_i, pH 7.0, 30 mM EDTA, 10% glycerol (w/v), 1 mM PMSF, 1/100 volume of methyltransferase crude extract]. The reactions were carried out at room temperature for 30−40 min and stopped by freezing in liquid nitrogen.

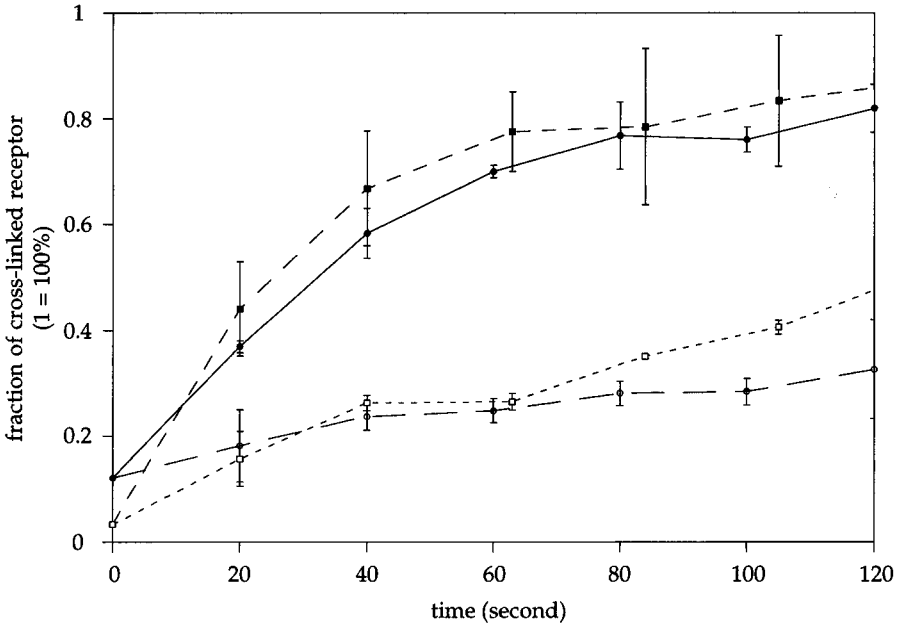

FIGURE 3: Cross-linking time courses of the N36C and T264C mutants in the presence and absence of aspartate. The mutant receptors were radiolabeled by *in vitro* methylation. Closed symbols, + aspartate; open symbols, − aspartate; uninterrupted line, N36C+asp; dashed line, N264C+asp; dotted line, T264C-asp; long dashes in line, N36C-asp.

Cross-Linking Kinetics of the Cysteine Mutants. The excess radioactive AdoMet and methyltransferase from methylation labeling reactions, and DTT from membrane preparations were removed from the membranes by centrifugation. The membranes were resuspended in final buffer (50 mM Tris-HCl, pH 7.5, 10% glycerol, 5 mM EDTA, 1 mM PMSF). They were preincubated at 37 °C for 5 min before the initiation of the cross-linking reactions triggered by 1 mM (final concentration) copper-phenanthroline. The whole reaction process was at 37 °C. At various time points (1, 2, 3, 4, 5, 10, 15, 30, and 60 min), the reaction mixture was aliquoted out and added to SDS sample buffer with 10 mM NEM (to block the free thiol groups) and 10 mM EDTA (to chelate cupric ions), and frozen immediately in liquid nitrogen. The cross-linked and uncross-linked receptors were separated on a 7.5% SDS gel. The appropriate bands were cut out, treated with 5 N NaOH at 37 °C for at least 20 h, to hydrolyze methyl ester. The volatile product, tritiated methanol, was absorbed by scintillation fluid, and the radioactivity was measured in a scintillation counter.

Data Processing. Equation 1 below (Careaga & Falke, 1992) was used to fit the data points in the cross-linking time courses to determine the k_{ss} and k_2 values. Under the

$$F_{ss}(t) = k_{ss}(1 - e^{-(k_{ss} + k_2)t})/(k_{ss} + k_2) \quad (1)$$

$$F_{ss}(\infty) = k_{ss}/(k_{ss} + k_2) \quad (2)$$

oxidation conditions with copper phenanthroline, two cysteine residues can form a disulfide bond, or be oxidized to sulfonic or sulfinic acid. The rate constant for disulfide formation is defined as k_{ss}, whereas that for the side oxidation reaction is k_2. The extent of disulfide formation, F_{ss}, as a function of time, is affected by both rate constants, in a manner as shown in Scheme 1 and eq 1. As time approaches infinity, eq 1 is converted to eq 2.

Fourier Transform and Least-Squares Transform. The mathematical methods were applied to detect any regularity of the hydrophobicity values of the region. This phenomenon was studied according to Cornette et al. (1987). Several hydrophobicity scales, including PRIFT, PRILS, ALTFT, ALTLS, TOTFT, and TOTLS (Cornette et al., 1987), as well as the Kyte−Doolittle scale (Kyte & Doolittle, 1982) were used in these analyses.

Scheme 1

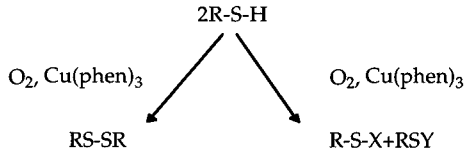

RESULTS

Figure 2 shows the single-cysteine mutants used in this study. Every residue from position 259 to 290 of the *S. typhimurium* aspartate receptor was mutated to a cysteine by site-directed mutagenesis. The membrane samples were prepared from each of these mutants, and the aspartate receptor in the membrane was radiolabeled by *in vitro* methylation. The cross-linking was carried out as described previously (Chen & Koshland, 1995).

Figure 3 shows the cross-linking time courses of the N36C mutant (from the periplasmic domain) and the T264C mutant from the cytoplasmic domain. The cross-linking rate of the T264C mutant is 0.34%/s, twice that of the N36C mutant (0.15%/s). In the presence of aspartate, both reactions became so rapid that rates were difficult to measure. Since the N36C mutant has been shown to form an inter-subunit cross-link within a functional dimer in previous cross-linking studies (Falke & Koshland, 1987), as well as in the crystal structure (Milburn et al., 1991; Scott et al., 1993), it is highly likely that the cross-links in the linker region are similarly juxtaposed.

In considering cross-linking rates of residues and their relations to an α-helix, Figure 4 is illustrative. Shown in that figure are two helices that are about one helix apart. If arranged on a rotation axis and the residues are labeled as a, b, c, d, e, f, g in two parallel helices, aligned as shown, residues a and a′ will be close to each other at a level from

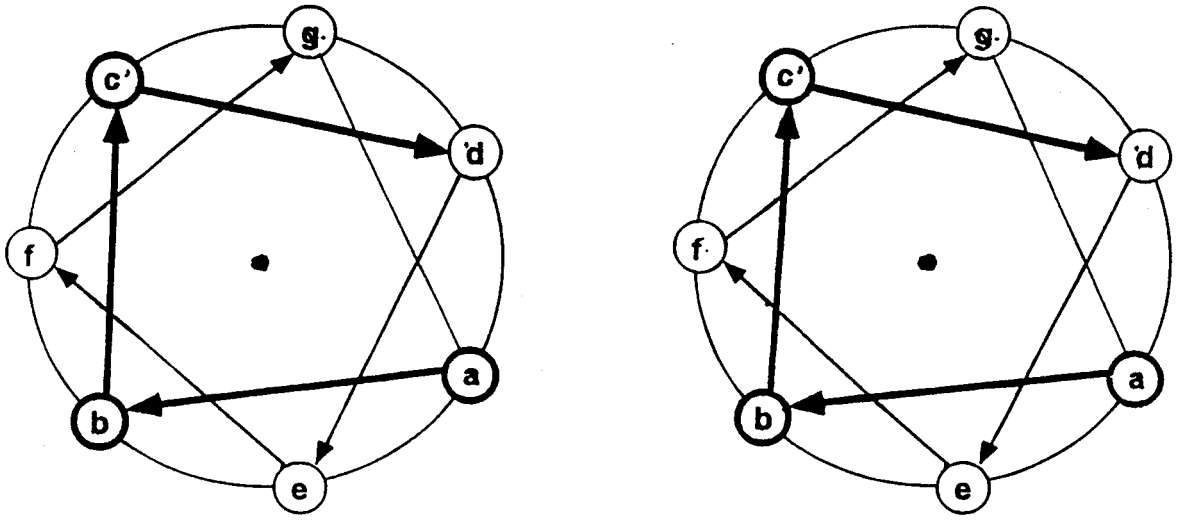

FIGURE 4: Schematic illustration of two helices of 3.6 residues per turn and radii of 1.0 units in which the centers of the two parallel helices are 2.84 units apart. In such a case the distances between residues in units are as follows: a−a′ = 1.48, b−b′ = 4.47, c−c′ = 4.37, d−d′ = 1.41, e−e′ = 3.21, f−f′ = 4.8, and g−g′ = 3.13. The distances apart of the two helices are approximately those observed in a number of proteins such as phosphorylase. It is assumed that a and a′ are level with each other on a plane perpindicular to the helix axis, and thus all the other residues b-b′, c-c′, etc. are also level with each other although at a different level from a-a′.

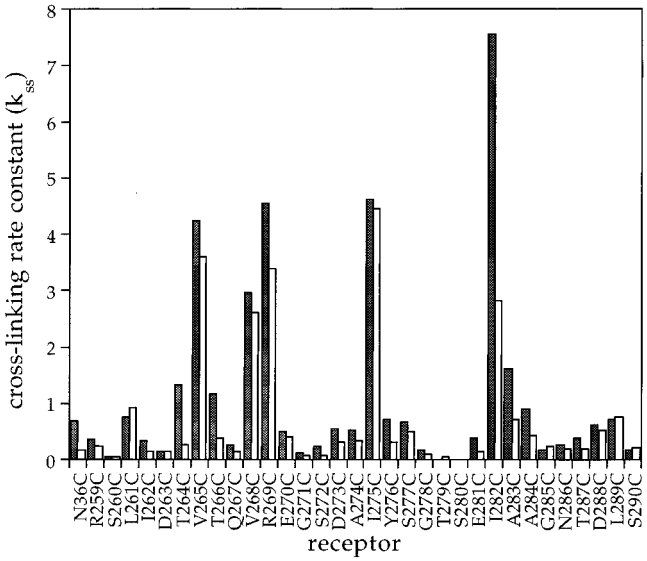

FIGURE 5: Rate constants for disulfide formation (k_{ss}) in the presence and the absence of aspartate. Cross-hatched, + aspartate; unfilled, − aspartate.

mutant	k_{ss} (+ asp)	k_{ss} (- asp)	mutant	k_{ss} (+ asp)	k_{ss} (- asp)
N36C	0.68	0.17	A274C	0.51	0.34
R259C	0.37	0.24	I275C	4.61	4.45
S260C	0.06	0.06	Y276C	0.71	0.31
L261C	0.76	0.93	S277C	0.66	0.51
I262C	0.32	0.16	G278C	0.16	0.09
D263C	0.16	0.14	T279C	0.00	0.04
T264C	1.34	0.25	S280C	0.01	0.01
V265C	4.25	3.59	E281C	0.38	0.14
T266C	1.17	0.38	I282C	7.56	2.81
Q267C	0.27	0.16	A283C	1.62	0.72
V268C	2.96	2.62	A284C	0.91	0.42
R269C	4.55	3.38	G285C	0.18	0.23
E270C	0.50	0.41	N286C	0.26	0.19
G271C	0.11	0.08	T287C	0.38	0.20
S272C	0.23	0.06	D288C	0.61	0.52
D273C	0.54	0.31	L289C	0.71	0.77
			S290C	0.18	0.22

FIGURE 6: Effect of aspartate on cross-linking rate constants. Cross-linking rate at various positions in cysteine mutants of the cytoplasmic domain of the aspartate receptor. In each case the cysteine was substituted in the amino acid position *n* indicated and the rates of the cross-linking between *n* and *n*′ in the adjacent subunits are recorded in the presence and absence of aspartate.

the bottom of the helix we shall call "level 1"; b and b′ will be far away from each other at level 2, c and c′ not close at level 3, and d and d′ essentially as close to each other as a and a′, but at level 4. Residues e and e′ will then be further apart than a-a′ and d-d′ but less far than b-b′ and c-c′ and at level 5. Thus there would be expected to be periodicity in cross-linking rates between *n* and *n*′ at intervals of between 3 and 4 residues apart in a helix.

Many mutants, e.g. T264C, V265C, V268C, R269C, G271C, S272C, I275C, I282C, and L289C, were cross-linked to a final extent of 90%. Many of these mutants had very high cross-linking rate constants (k_{ss}).

The rate constants for side reactions (k_2) are generally very small when the k_{ss} values of the same mutant are very large. It has been observed in the previous studies on ribose/galactose binding protein (Careaga & Falke, 1992), the k_2/k_{ss} values determined experimentally using purified protein were very similar to those extrapolated from the equations used here.

When the cross-linking data were compared with the hydrophobicity profile (Figures 6 and 7), it was found that the positions of maximal cross-linking rates were the same as those of maximal hydrophobic values. In order to assess the cross-linking data and the hydrophobicity values of the residues in this region more objectively, Fourier transforms and least-square fit were performed to detect the potential regularity of the data. As shown in Figure 6, both transformation methods displayed a prominent peak around 105°, for both the hydrophobicity indices and the k_{ss} values. Several different hydrophobicity scales (listed in Materials and Methods) were used to see the variation within the display which could be caused by the different scales one chooses. The average frequency at which the predominant peak was observed was 104.7 ± 1.0°. This is an indication of an amphiphilic α-helix (Eisenberg et al., 1982; Cornette et al., 1987).

The rate constants of disulfide formation (k_{ss}) of the L261C, V265C, V268C/R269C, I275C, I282C, and L289C mutants were higher than those of their immediate neighbors on either side, respectively, whereas the D263C, Q267C, and G271C mutants had lower cross-linking rate constants (k_{ss})

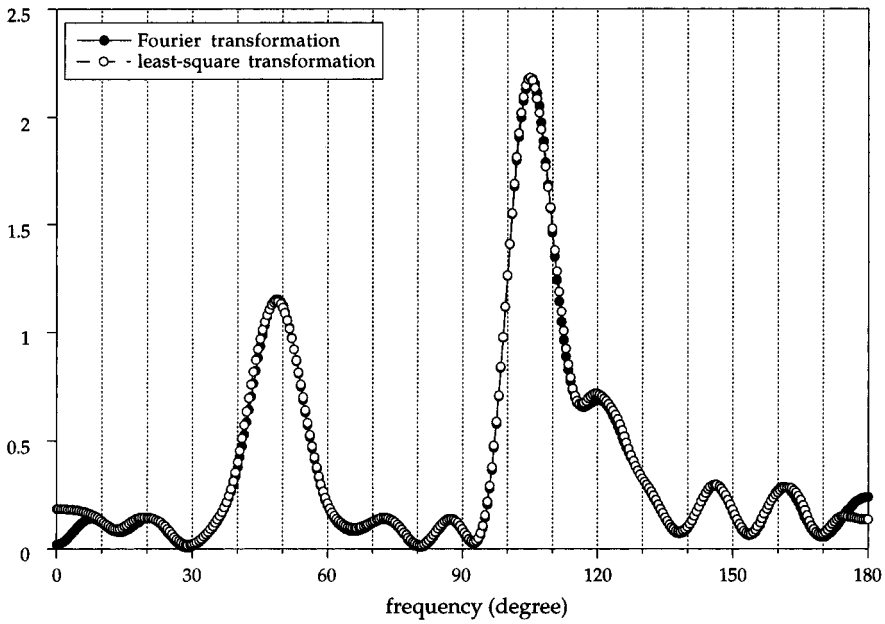

FIGURE 7: Fourier transform and least-squares transform power spectra of the hydrophobicity values of residues 260−289. Several different hydrophobicity scales were used (see Materials and Methods for details). Only the spectra based on the PRIFT scale are shown here. Values on similar scales did not differ from these significantly. The average value of the frequency corresponding to the peak in power spectrum was 104.7 ± 1°. FT, Fourier transform; LS, least-squares transform.

than their immediate neighbors on either side, respectively (Figure 5).

The addition of aspartate led to an increase in the k_{ss} values for all of the mutants (Figure 6).

The cross-linking rates in the cytoplasmic domain give clear evidence of a juxtaposition of the regions 259−282 and 259′-282′. That juxtaposition indicates the way the cytoplasmic domain is structured relative to the periplasmic domain. In Figure 8a is seen the orientation of helices 1 and 4 in the periplasmic domain as seen from an observer looking down the helices toward the membrane. Residues along helices 1 and 1′ are close, and this conclusion is supported by cross-linking data in the helical regions that extend into the membrane as TM1 and TM1′ (Lynch & Koshland, 1991; Jeffrey & Koshland, 1993; Milligan et al., 1988) and by X-ray crystallography (Milburn et al., 1991). Residues in helix 4 that become transmembrane domains 2 and 2′ are farther apart and cannot have the rapid cross-linking rates of TM1 or TM1′ residues. This leads to the hypothesis that the structure of the cytoplasmic domain must show some feature like Figure 8 and not be a a simple straight extension of the 4 helices of TM1, TM2, TM1′, and TM2′ (Figure 8). Moreover, they must continue as parallel sequences not antiparallel.

The addition of aspartate in the cross-linking studies increased both the rate and final extent of disulfide bond formation (Figure 5). This can be achieved by a conformational change in the cytoplasmic domain of the receptor which brings the two helices closer together within an already-existing dimer. The conformational change is transmitted to the linker region of the receptor, in such a way that all of the residues along this region changed into a better juxtaposition for disulfide bond formation. This conformational change does not cause a shift in the relative positions of the residues with changing local maximal or minimal cross-linking rate constants. Thus, a global rotational model (Maruyama et al., 1995) extending to the cytoplasmic domain as the mechanism of aspartate receptor-mediated transmembrane signaling seems unlikely. If a global rotation occurs as a result of aspartate binding, one would expect that such a shift would cause some shift in relative rates at different amino acid residues. For example, the cross-linking rate of T266C mutant might increase and that of V265C might decrease, resulting in a peak shift from position 265 to 266, at least partially.

The Fourier transform method was originally designed to detect any periodicity of the distribution of hydrophobic residues within a given sequence (Cornette et al., 1998, and references therein). Ideally, a Fourier transform power spectrum would peak at a frequency of 100° for an α-helix of 3.6 residues per turn. It has been applied to the random mutagenesis results of the aspartate receptor transmembrane regions (Maruyama et al., 1995) and the cross-linking results of the corresponding regions of the ribose/galactose receptor (Lee & Hazelbauer, 1994). In this study, a predominant peak was observed at 105°, for the hydrophobicity values of the wild type residues, as well as the cross-linking rate constants of the cysteine mutants within this region. This is an indication of an α-helical conformation.

DISCUSSION

Two features of the structure of the cytoplasmic domain stand out: (a) The two linker regions appear to be very close to each other and (b) the amino acid sequences of the linker region are parallel to each other. The closeness is indicated by the rapidity of disulfide cross-linking. For example, 265 or 265′ has a rate constant of 3.5 in the absence of aspartate, and the rate constant for 36−36′ cross-linking is 0.2 in the absence of aspartate. Residues 36 and 36′ are known to be very close together from the X-ray structure of the periplasmic domain (Milbern et al., 1991). The 36−36′ mutant forms the cross-link very rapidly and the cross-linked structure retains transmembrane signaling (Falke & Koshland, 1987). Thus it is surprising that cysteines inserted at residues 265, 268, 269, and 275 react even faster than 36−36′.

Since these residues react rapidly, the two sequences must be quite parallel, otherwise one of the mutants would put

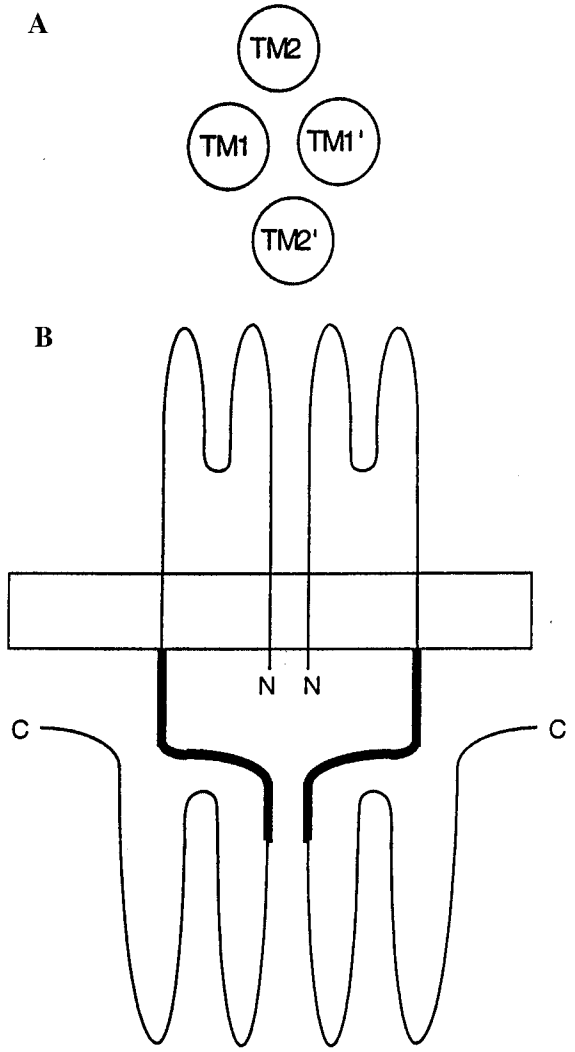

FIGURE 8: (a) Positions of transmembrane domains as projections from helices 1 and 4 of the periplasmic domain of the aspartate receptor. Assuming straight projection of α-helices, transmembrane regions 1 and 1′ are close, 2 and 2′ regions are further apart. (b) Postulated structure of the cytoplasmic domain based on targeted disulfide cross-linking data. Helices 2 and 2′ are bent to bring sequences of 261−275 close to sequence 261′−275′. The linker region (shown as the heavy line) is defined here as the residues from the membrane to the methylation site (residues 213−294). The portion studied here is from residue 261 to residue 275.

residues *n*, *n*′ very close but residues $(n + x)$, $(n + x)'$ or $(n - x)$, $(n - x)'$ would certainly have k_{ss} rates that decrease rapidly as their distance from each other would get larger and larger.

A second conclusion also appears likely. The residues appear to be α-helical in general. There is a periodicity in reactivity of the cysteine mutants, as illustrated in Figure 5, suggesting a helical wheel as indicated in Figure 4. However, the periodicities are not as crisp and clear as one might expect for perfect helices in parallel juxtaposition. So it appears that there is not a perfect helical arrangement and that the orientation of the helical regions is parallel in general but leaves some less helical stretches. This is perhaps surprising because the sequence indicator is that the region is quite helical and circular dichrosism indicates high helical content.

The seven-residue repeating pattern between 261, 268, 275, 282, and 289 is reminiscent of a coiled-coil conformation adopted by many proteins. The most distinctive feature of a coiled coil is a heptad repeat (denoted as abcdefg), where residues at positions a and d are most hydrophobic. The stability of such a structure is maintained by the hydrophobic interactions between positions a and d and electrostatic interactions between positions e and g. If the positions are assigned to the residues studied in this region, it is found that most of the a and d positions are occupied by hydrophobic residues, but the residues at positions e and g are not consistent with the theory above. The pattern has some elements of a helical structure but also some indication of less regular structures.

It is also apparent that there appears to be little rotation caused by the addition of aspartate. Aspartate appears to draw the two subunits closer together (Figure 5), as also observed for the periplasmic domain (Milligan & Koshland, 1988). The rate constants for cross-linking increase for every residue on addition of aspartate, some very dramatically, *e.g.*, residue 264, 0.2 in absence of aspartate and 1.3 in the presence of aspartate, and less dramatically in others, *e.g.*, residue 262, 0.2 in the absence and 0.3 in the presence. However, large rotation does not seem to be occurring since such an event would be expected to increase rates of some residues and decrease rates of some adjacent residues.

Some of the patterns of peaks and valleys are explainable on a parallel helices assumption, but others are not. Peaks at 265 and 268 are explainable on the basis of Figure 4 if 265 is at an *a* position and then 268 would be expected to be at the *d* position. Since both a−a′ and d−d′ would be close on a parallel helices plot, both should cross-link rapidly as is observed. Likewise, 265 and 275 cross-links would give 265−265′ as a-a′ positions and 275−275′ at d and d positions, both close. Such a pairing would however put 269 and 269′ at b and b′ positions that would be expected to react more slowly and yet 269−269′ is found to form rapidly. On balance, parallel helices seem likely but not absolutely definitive.

There does appear to be considerable flexibility in the protein conformation indicating some ability to rotate through various conformations spontaneously. In Figure 4 are shown two helices separated by about the width of one helix (not an unusual distance for helices in known proteins). As can be seen, the distances between *n* and *n*′ can be rather similar to those between $(n + 3)$ and $(n + 3)'$, when *n* is in the a position and $n + 3$ is in the d position. However, if the helices are lined up in this manner, one would expect a quite severe drop in rate for helices when $n-n'$ equals a−a′ and $(n + 1)-(n + 1)'$ are b−b′. Thus it is surprising that 268−268′ and 269−269′ are equally fast. Moreover, other situations can place helices so that *n* and *n*′ are very close and both $(n + 1)$ and $(n + 1)'$ and $(n - 1)$ and $(n - 1)'$ are apparently further from each other. That seems to be the case for 275−275′, where cross-linking is very rapid and for 274−274′, 267−267′, where cross-linkings are very much slower.

In summary the targeted disulfide technique appears to generate interesting and important information about the structure of the cytoplasmic domain, but it leaves some puzzling phenomena that may only be resolved when the X-ray structure of this domain is solved.

REFERENCES

Ames, P., & Parkinson, J. S. (1988) *Cell 55*, 817−826.

Biemann, H. P., & Koshland, D. E., Jr. (1994) *Biochemistry 33*, 629−634.

Bollinger, J., Park, C., Harayama, S., & Hazelbauer, G. L. (1984) *Proc. Natl. Acad. Sci. U.S.A. 81*, 3287−3291.
Boyd, A. W., Kendall, K., & Simon, M. I. (1983) *Nature 301*, 623−626.
Careaga, C. L., & Falke J. J. (1992) *J. Mol. Biol. 226*, 1219−1235.
Chen, X., & Koshland, D. E., Jr. (1995) *J. Biol. Chem. 270*, 24038−24042.
Chervitz, S. A., & Falke J. J. (1995) *J. Biol. Chem. 270*, 24043−24053.
Chervitz, S. A., Lin, C. M., & Falke J. J. (1995) *Biochemistry 34*, 9722−9733.
Cornette, J. L., Cease, K. B., Margalit, H., Spouge, J. L., Berzofsky, J. A., & DeLisi, C. (1987) *J. Mol. Biol. 195*, 659−685.
Eisenberg, D., Weiss, R. M., & Terwilliger, T. C. (1982) *Nature 299*, 371−374.
Falke, J. J., & Koshland, D. E., Jr. (1987) *Science 237*, 1596−1600.
Falke, J. J., Dernburg, A. F., Sternberg, D. A., Zalkin, N., Milligan, D. L., & Koshland D. E., Jr. (1988) *J. Biol. Chem. 263*, 14850−14858.
Foster, D. L., Mowbray, S. L., Jap, B. K., & Koshland, D. E., Jr. (1985) *J. Biol. Chem. 260*, 11706−11710.
Gardina, P., & Manson, M. (1996) *Science 274*, 425−426.
Jancarik, J., Scott, W. G., Milligan, D. L., Koshland D. E., Jr., & Kim, S.-H. (1991) *J. Mol. Biol. 221*, 31−34.
Jeffery, C. J., & Koshland, D. E., Jr. (1994) *Biochemistry 33*, 3457−3463.
Kobashi K. (1968) *Biochim. Biophys. Acta 158*, 239−245.
Krikos, A., Mutoh, N., Boyd, A. W., & Simon, M. I. (1983) *Cell 33*, 615−622.
Kunkel, T. A. (1985) *Proc. Natl. Acad. Sci. U.S.A. 82*, 488−492.
Kyte, J., & Doolittle, R. F. (1982) *J. Mol. Biol. 157*, 105−132.
Lee, G. F., & Hazelbauer, G. L. (1995) *Protein Sci. 4*, 1100−1107.
Lee, G. F., Burrows, G. G., Lebert, M. R., Dutton, D. P., & Hazelbauer, G. L. (1994) *J. Biol. Chem. 269*, 29920−29927.
Lee, G. F., Dutton, D. P., & Hazelbauer G. L. (1995a) *Proc. Natl. Acad. Sci. U.S.A. 92*, 5416−5420.
Lee, G. F., Lebert, M. R., Lilly, A. A., & Hazelbauer, G. L. (1995b) *Proc. Natl. Acad. Sci. U.S.A. 92*, 3391−3395.
Lee, J., & Pilch, P. (1994) *Am. J. Physiol. 94*, C319−C334.
LeMoual, H., & Koshland, D. E., Jr. (1996) *J. Mol. Biol. 261*, 568−585.
Lynch, B. A., & Koshland D. E., Jr. (1991) *Proc. Natl. Acad. Sci. U.S.A. 88*, 10402−10406.
Lynch, B. A., & Koshland, D. E., Jr. (1992) *FEBS Lett. 307*, 3−9.
Maruyama, I. N., Mikawa, Y. G., & Maruyama, H. I. (1995) *J. Mol. Biol. 253*, 530−546.
Milburn, M. V., Prive, G. G., Milligan, D. L., Scott, W. G., Yeh, J., Jancarik, J., Koshland, D. E., Jr., & Kim, S.-H. (1991) *Science 254*, 1342−1347.
Milligan, D. L., & Koshland, D. E., Jr. (1988) *J. Biol. Chem. 263*, 6268−6275.
Milligan, D. L., & Koshland, D. E., Jr. (1991) *Science 254*, 1651−1654.
Moe, G. R., Bollag, G. E., & Koshland, D. E., Jr. (1989) *Proc. Nat. Acad. Sci. U.S.A. 86*, 5683−5687.
Mowbray, S. L., & Koshland, D. E., Jr. (1987) *Cell 50*, 171−180.
Mowbray, S. L., Foster, D. L., & Koshland, D. E., Jr. (1985) *J. Biol. Chem. 260*, 11711−11718.
Mutoh, N., Oosawa, K., & Simon, M. I. (1986) *J. Bacteriol. 167*, 992−998.
Oosawa, K., & Simon, M. (1986) *Proc. Natl. Acad. Sci. U.S.A. 83*, 6930−6934.
Pakula, A. A., & Simon, M. I. (1992) *Proc. Natl. Acad. Sci. U.S.A. 89*, 4144−4148.
Russo, A. F., & Koshland, D. E., Jr. (1983) *Science 220*, 1016−1020.
Sahin-Toth, M., & Kaback, H. R. (1993) *Protein Sci. 2*, 1024−1033.
Scott, W. G., & Stoddard, B. L. (1994) *Structure 2*, 877−887.
Scott, W. G., Milligan, D. L., Milburn, M. V., Prive, G. G., Yeh, J., Koshland, D. E., Jr., & Kim, S.-H. (1993) *J. Mol. Biol. 232*, 555−573.
Shapiro, M. J., & Koshland, D. E., Jr. (1994) *J. Biol. Chem. 269*, 11054−11059.
Sorokin, A., Lemmon, M. A., Ullrich, A., & Schlessinger, J. (1994) *J. Biol. Chem. 269*, 9752−9759.
Stoddard, B. L., Bui, J. D., & Koshland, D. E., Jr. (1992) *Biochemistry 31*, 11978−11983.
Tatsuno, I., Houma, M., Oosawa, K., & Kawagishi, I. (1996) *Science 274*, 423−425.
Weitzman, C., & Kaback, H. R. (1995)*Biochemistry 34*, 9374−9379.
Wolfe, A. J., Conley, M. P., & Berg, H. C. (1988) *Proc. Natl. Acad. Sci. U.S.A. 85*, 6711−6715.
Wu, J., Li, J., Li, G., Long, D. G., & Weiss, R. W. (1996) *Biochemistry 35*, 4984−4993.
Yamamota, K., & Imae, Y. (1993) *Proc. Natl. Acad. Sci. U.S.A. 90*, 217−221.
Yeh, J. I., Biemann, H. P., Pandit, J., Koshland, D. E., Jr., & Kim, S.-H. (1993) *J. Biol. Chem. 268*, 9787−9792.

BI970911U